Droplet Impingement into a Liquid Film; Numerical Study of Surface Tension Effect on the Crown Formation

Mohammad Mehdi Zamani Asl* and Zahra Dastyar

Department of Mechanical Engineering, Shahid Chamran University of Ahvaz, Ahvaz, Iran
E-mail: mzamaniasl@gmail.com
**Corresponding Author*

Received 20 August 2021; Accepted 04 January 2022;
Publication 21 January 2022

Abstract

An axisymmetric numerical model is conducted to study the droplet impingement into a liquid film and crown formation. Through numerical modeling and experimental validation, the effect of different parameters such as surface tension, Weber number, and film thickness on crown evolution is investigated. Surfactant is added to water, aiming reduction of the surface tension in the surfactant-water mix. It was shown that the crown rim diameter increases with Weber in both water and surfactant-water mixture cases. Likewise, crown rim diameter increases with the film thickness in both different cases of fluids.

Additionally, results revealed that surface tension does not affect the crown rim diameter. Nevertheless, crown height increases as surface tension decreases. At low values of surface tension, secondary droplets and the dewetting region appear. These outcomes can be attributed to the domination of kinetic energy of crown rims in cases with low surface tensions.

Keywords: Numerical study, crown formation, droplet impact, surface tension, liquid film, Weber number.

European Journal of Computational Mechanics, Vol. 30_4–6, 519–536.
doi: 10.13052/ejcm2642-2085.304610

1 Introduction

Droplet impact is a prevalent phenomenon in nature and a variety of industries. Impingement of liquid droplets on different surfaces and their outcomes have been studied widely due to their natural complexity and industrial applications. Fuel injection, inkjet printers, and spray cooling are examples of droplet impact applications on industrial scales. Since the droplet impact process outcomes can affect the industrial systems and their performances or even induces imperfections in the systems, knowing these processes' outcomes and underlying physics is vital for enhancing performances or minimizing potential faults [1, 2].

Droplet impact on a liquid surface has been studied extensively owing to its distinct post-impact outcomes. The jet breakup was explored in experimental work for water and methoxy-nonafluorobutane liquids over the range of impact velocities. The result revealed a jet breakup for water drop impacting water liquid film, suggesting a critical Weber number for the water-water case. However, no jet breakup is reported for the water-methoxy case over the range of impact velocities, which indicates no critical Weber number for this case [3]. The crown formation, crown-splash, and crown-deposition limits are generally described by two variable parameters of the impact process: the dimensionless film thickness ($H^* = h/d$) and K parameter ($K = We \cdot Oh^{0.4}$). For the high values of the K parameter, which means at higher inertia, splashing occurs. In the low values of K, however, the inertia is not strong enough to create a crown. Thus, only deposition can be seen. For the mediocre values of K, inertia is strong enough to create a crown but not enough to induce splashing. For a particular value of dimensionless film thickness ($H^* < 0.02$), crown formation without splashing is no longer observed [4].

Deegan et al. [5] examined the drop impact on a deep pool with a significant focus on the ejecta sheet and Lamela layer evolution. While the ejecta sheet and Lamela layer are considered one phenomenon in previous studies, Deegan illustrated that the ejecta sheet and Lamela layer are different. Nonetheless, for low Re, ejecta and Lamela sheets merge and create single ejecta. By increasing the Re and We, ejecta and Lamela sheets can be distinguished. Effects of film viscosity and ambient gas pressure on ejecta sheet and splash outcomes of drop impact have been investigated by Marcotte et al. [6]. He showed that a splash's downward curve would change into an upward curve by increasing the liquid film viscosity. He also reported that decreasing the ambient air pressure suppresses the splash and crown formation. However,

further studies could have been done on impact outcomes at lower impact velocities. The controlling mechanism of suppression behavior at lower ambient gas pressure has not been discussed adequately. Impact at higher ambient gas could have been another interesting subject to investigate.

Che et al. [7] studied the effect of surface tension on drop impingement and crown formation afterward. He analyzed the crown formation process for different pure water drop and film liquids and water drop and film liquids with surfactant additives. Surfactant has been used to reduce the surface tension in liquids. It has been revealed that by adding a surfactant, crowns form with more stabilized rims, which grow almost vertically, and the number of secondary droplets decreases. The presence of surfactants also alters the propagation of after impact capillary waves. In cases of surfactant drop impacting water film, capillary waves move faster due to surface tension gradient in the impact region and other parts of the liquid film.

Air entrainment and air film rapture during the drop impact on a deep pool have been described by Tran [8]. During the impact process, air film thickness between the drop and liquid pool decreases until it reaches a certain level and eventually ruptures. Rupture position was noticed to be dependent on impact velocity and fluid viscosity. Additionally, Tran derived a scaling law for the rupture position, which takes airflow in the film into consideration.

Moreover, many numerical studies have been implemented to investigate the droplet impact process and outcomes. Xie et al. [9] employed the particle method to model the crown formation during the drop impact process. A numerical model is conducted by Guo et al to simulate the high-speed droplet impact process. A comparison with the experimental results showed that they could model the interfaces accurately [10]. Agbaglah [11] simulated the drop impact into a deep pool. They captured the ejecta sheet and jet formation in their simulation, which was their work's main idea. Y. Guo et al. [12] used a coupled method of Volume of Fluid (VOF) and Level set to simulate the droplet impact into a liquid film. They analyzed the effect of impact velocity and liquid film thickness on the spreading process. They mentioned that as the liquid film increases, the spreading diameter decreases. Many studies have been done about the different parameters in the droplet impact process and outcomes of this process-such as impact velocity effect, viscosity effect, and effect of film thickness. Nonetheless, the surface tension effect is less investigated experimentally and numerically, which shows the significance of this work.

This study aims to simulate the droplet impingement into a liquid film of water and the crown formation and effect of Weber number, film

thickness, and droplet size on the crown diameter during the impact process. The surfactant has also been added to water to explore the crown formation and evaluation's surface tension effect. This study's primary focus is the high Weber number (high velocity) impacts that produce the Crown at different states.

2 Numerical Methods

Droplet impact into a liquid film is a two-phase flow that contains liquid (water) and gas (air) phases. The following assumptions are made to simulate this flow:

- Laminar flow regime
- Incompressible flow with Newtonian fluids
- Constant fluid properties (density, viscosity, etc.) during the entire process
- Droplet shape is spherical during the impact

2.1 Governing Equations

In multiphase flows, the interface is the critical point where different phases interact, and these interactions change the interface shapes. Coupled level-set & Volume of Fluid (CLSVOF) method is a multiphase flow model consisting of Volume of Fluid (VOF) and Level-set methods. This method can model the interfaces and fluid phases accurately. Considering that the VOF method is discontinuous across the interfaces, the Level-set method can model the interfaces effectively since the level set offers smooth change and continuity across the interfaces. Therefore, the coupling Level-set and VOF method is an efficient way to model the multiphase flows [13].

Mass and Momentum equations can be written as:

$$\frac{\partial \varphi}{\partial t} + \mathrm{u} \cdot \nabla \varphi = 0 \tag{1}$$

$$\frac{\partial (\rho u)}{\partial t} + \nabla \cdot (\rho u u) = -\nabla P + \nabla \cdot \widetilde{\tau} + \overrightarrow{F}_{sf} + \rho \overrightarrow{g} \tag{2}$$

The surface tension force ($\overrightarrow{F}_{sf}$) is evaluated as below:

$$\overrightarrow{F}_{sf} = \sigma k \delta(\varphi) \overrightarrow{n} \tag{3}$$

Where σ, k, $\delta(\varphi)$ and $\vec{n}$ are surface tension coefficient, local mean interface curvature, dirac function, and local interface normal.

The density (ρ) and viscosity (μ) of each fluid are constant. Thus, discontinuity is observed in interfaces for each of these physical properties. To smoothen the discontinuity, using the heaviside function, density, and viscosity is defined as [14]:

$$\rho(\varphi) = \rho_l H(\varphi) + \rho_g(1 - H(\varphi)) \tag{4}$$

$$\mu(\varphi) = \mu_l H(\varphi) + \mu_g(1 - H(\varphi)) \tag{5}$$

The heaviside function is defined as:

$$H(\varphi) = \begin{cases} 0 & \text{if } \varphi < -a \\ \frac{1}{2}\left(\frac{\varphi + a}{a} + \frac{1}{\pi}\sin\left(\pi\frac{\varphi}{a}\right)\right) & \text{if } |\varphi| \le a \\ 1 & \text{if } \varphi > a \end{cases} \tag{6}$$

The dirac function can be written as:

$$\delta(\varphi) = \frac{\partial H(\varphi)}{\partial \varphi} \tag{7}$$

$$\delta(\varphi) = \begin{cases} 0, & |\varphi| > a \\ \dfrac{1 + \cos\left(\frac{\pi\varphi}{a}\right)}{2a}, & |\varphi| \le a \end{cases} \qquad (a = 1.5z) \tag{8}$$

Where z is the grid spacing and (φ) is the Level-set function which is determined as a signed distance from interfaces. The Level-set function is given as [15]:

$$\varphi(x,t) = \begin{cases} +|d|, & \text{the primary phase} \\ 0, & \text{the interface} \\ -|d|, & \text{the secondary phase} \end{cases} \tag{9}$$

Where d is the distance from the interface.

Local mean interface curvature and local interface normal are expressed as [16, 17]:

$$k = \nabla \cdot \frac{\nabla\varphi}{|\nabla\varphi|_{\varphi=0}} \tag{10}$$

$$\vec{n} = \frac{\nabla\varphi}{|\nabla\varphi|_{\varphi=0}} \tag{11}$$

2.2 Boundary Condition and Domain

A two-dimensional axisymmetric simulation is carried out. Figure 1 shows the schematic of the computational domain and boundary conditions. In this modeling, instead of a droplet falling because of gravitational force, the droplet will impact the film from the initial height of $h = 0.1D$, where D is droplet diameter and the initial speed of u. This initial height has been chosen so as not to affect the accuracy of the result.

The computational domain is chosen in a way to include the impact region mainly. Therefore, a rectangular field with a width of 4.75D and a height of 2.5D is generated where D is droplet diameter. In order to achieve a high-quality mesh, the adaptive refinement method has been conducted to create a better mesh grid in the liquid film and droplet impact regions (Figure 2). Thus, mesh size in the refined areas is equal to 1/200 droplet diameter. The grid study showed that the result does not change with the mesh grids, which are finer than 1/200 drop diameter.

The PISO method was used to couple the pressure and velocity. The Navier–Stokes equation and Level-Set function were solved by quadratic upwind interpolation of convective kinematics. The VOF function and Level-Set equation are solved by geo-reconstruction and MUSCL, respectively.

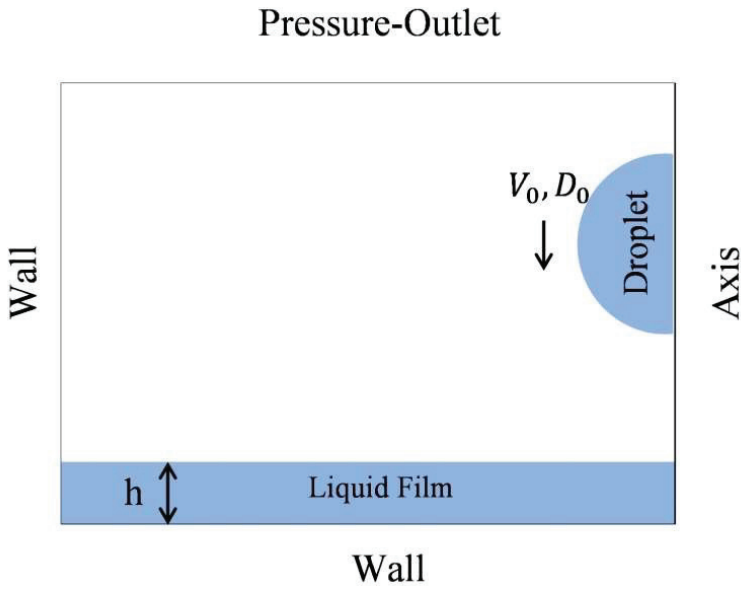

Figure 1 Schematic of droplet impact configuration, domain, and boundary conditions.

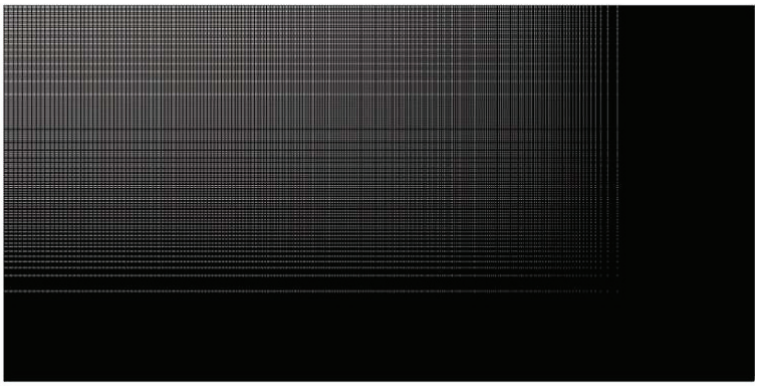

Figure 2 Schematic of the discretized domain.

3 Results and Discussion

The numerical result is validated against the experimental study of Che and Mattar [7]. Two different cases of fluids have been used in this simulation. In the first case, the film liquid and droplet are from dio-ionized water. The sodium dodecyl sulfate (SDS) has been added as a surfactant to dio-ionized water for the second case.

Since surfactant mixture properties are dependent on the concentration of surfactant in the solvent, the effect of surfactant on these properties must be considered. Critical micelle concentration (CMD) is defined as the concentration of surfactants above which micelles form, and all additional surfactants added to the system go to micelles. CMC is a critical parameter in determining surfactant properties. The surface tension of water decreases due to added surfactant in the water. The viscosity of surfactant mixtures will increases while surfactant concentration increases until surfactant concentration reaches the CMC. For the surfactant concentrations above the CMC, the viscosity decreases with increasing the concentration of the surfactant. SDS is a surfactant with a critical micelle concentration (CMC) of 8.2 mM. In Che's experiment, SDS is used at the 65.6 mM concentration, way above the CMC. Thus, the viscosity of the mixture slightly decreases by adding the SDS to dio-ionized water. In addition, viscosity changes are negligible. The added surfactant does not change the density of the mixture significantly. Thereby, the density of water will also remain constant [18, 19]. Table 1 shows the range of properties of dio-ionized water and the water-surfactant mixture.

Table 1 Fluids properties

Properties	Water	Surfactant-Water
σ (N/m)	0.071	0.0344
μ (Pa.s)	0.001	0.00082
ρ (Kg/m^3)	1000	1000

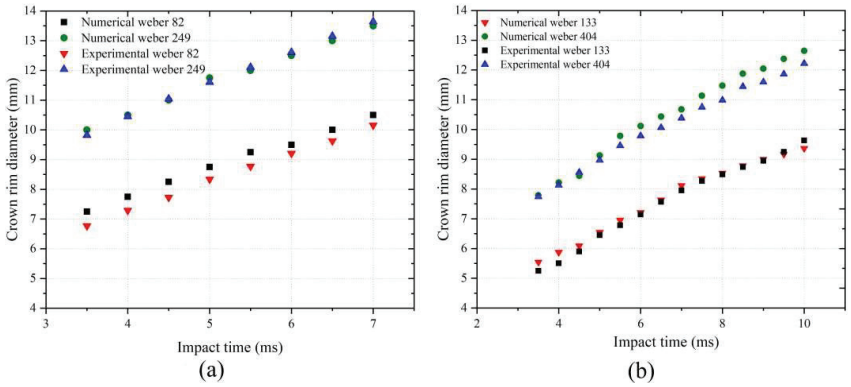

Figure 3 Crown rim diameter evolution vs. impact time at different Weber numbers in experimental and numerical cases; (a) water and (b) surfactant-water; droplet diameter and the film thickness is d = 3.15 mm, and h = 0.7 for case (a) and d = 2.47 mm and h = 0.7 for case (b), respectively.

3.1 Effect of Weber Number (We)

Weber number is a dimensionless number that represents the ratio of inertia and surface tension, and it is given below [20]:

$$We = \frac{\rho_{drop} u^2 d}{\sigma_{drop}} \tag{12}$$

Where ρ, u, d, and σ are droplet liquid density, impact velocity, droplet diameter, and surface tension of the droplet liquid, respectively.

Figure 3 shows the crown rim diameter's evolution at different Weber numbers for water and surfactant-water mixture cases. Experimental and numerical results are in good agreement. Crown rim diameter and crown height increase with Weber number in both water and surfactant-water cases. Inertia is a key factor in crown formation. The inertia will be transported to liquid film during the impact process, leading to the crown formation. Impacts with higher Weber numbers can be interpreted as higher inertia, and this higher inertia results in larger crown heights and rim diameters. With a

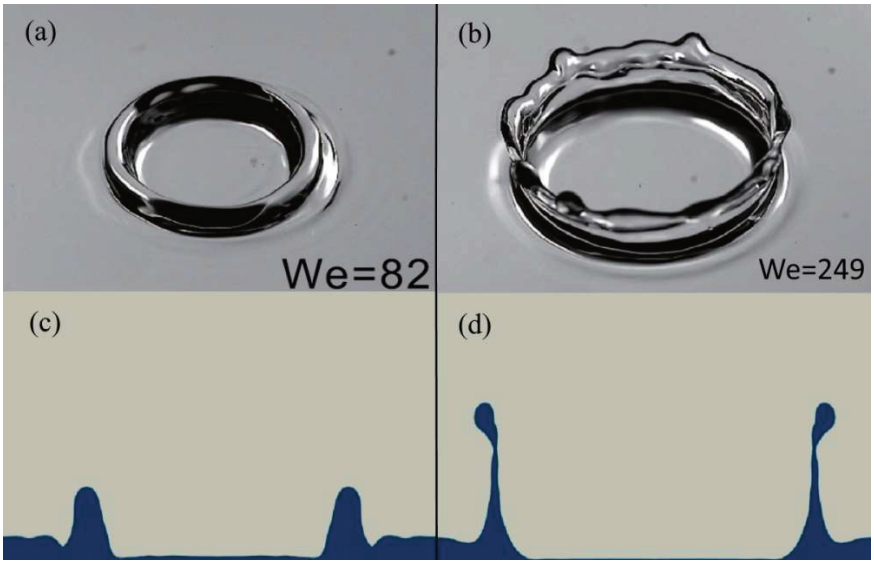

Figure 4 Weber number effect on droplet impact process and crown formation for water case; Snapshot of crown formation at t = 7 ms after impact; (a) experimental case with Weber number of 82 ($u = 1.4$ m/s) (b) experimental case with Weber number of 249 ($u = 2.4$ m/s) (c) numerical case with Weber number of 82 ($u = 1.4$ m/s) (d) numerical case with Weber number of 249 ($u = 2.4$ m/s); droplet diameter and the film thickness is d = 3.15 mm and h = 0.7 mm, respectively.

sufficiently large Weber number, the crown rim eventually forms a secondary droplet ring, which finally would be ejected from this ring [Figure 4]. The formation of these secondary droplets can be described as a competition between inertia and surface tension [21]. The interaction between kinetic energy (inertia) and surface tension in crown evolution will be discussed in the final section. It can also be seen that surface waves that propagate in the liquid film after impact are only noticeable in the water case, and the film beyond the Crown is flat and smooth in the surfactant-water case. However, these surface waves are primarily created in low Weber number cases.

3.2 Liquid Film Thickness Effect

The liquid film thickness is a critical parameter in the droplet impact process and crown formation. Crown rim and height reduce as the film thickness grows. Crown thickness alternatively elevates with the increment of the film thickness. Besides, the secondary droplets are eliminated or generated less

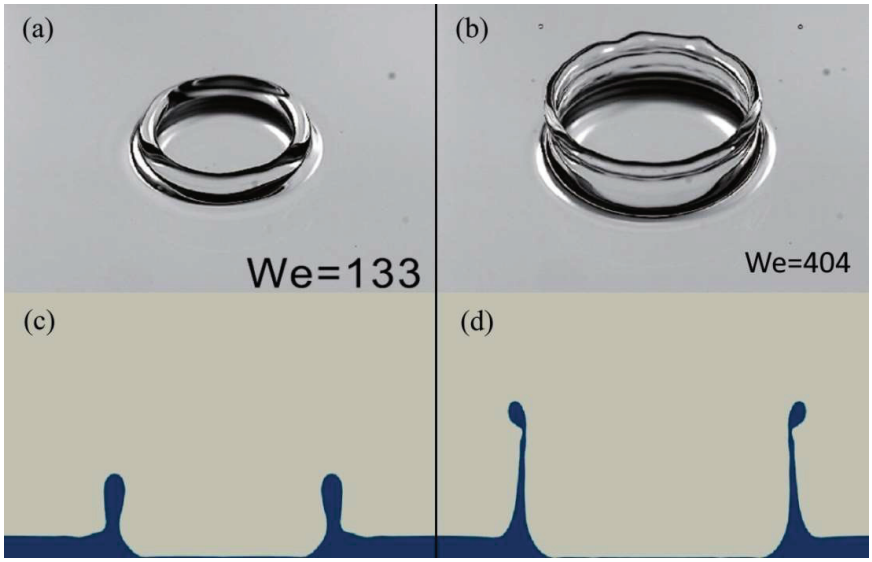

Figure 5 Weber number effect on droplet impact process and crown formation for surfactant-water mixture; Snapshot of crown formation at t = 7 ms after impact; (a) experimental case with Weber number of 133 ($u = 1.4$ m/s) (b) experimental case with Weber number of 404 ($u = 2.4$ m/s) (c) numerical water-water impact at Weber number of 133 ($u = 1.4$ m/s) (d) numerical water-water at Weber number of 404 ($u = 2.4$ m/s); droplet diameter and the film thickness is d = 2.47 mm and h = 0.7 mm, respectively.

often as film thickness increases. The elimination of secondary droplets stems from the fact that thicker film and subsequently thicker crowns are more stable, and instabilities cannot form necking points in the crown rim regions. Thus, secondary droplets are less common in the thick fluid films.

Crown evolution is slower in thick fluid films. The droplet has to overcome the resistance of film for crown formation. Since the thicker film needs larger inertia to form the Crown, with the same inertia (same Weber number), the Crown will develop slower in the thicker films. It grows faster in a thin film due to the slight resistance of the liquid film (Figure 6).

3.3 Effect of the Surface Tension

Three impact cases have been carried out with the same impact parameters and different surface tensions to properly investigate the surface tension effect on crown evolution. Figure 9 shows the snapshot of the surfactant-water mixture case with three surface tension coefficients. Figure 10(a) illustrates the

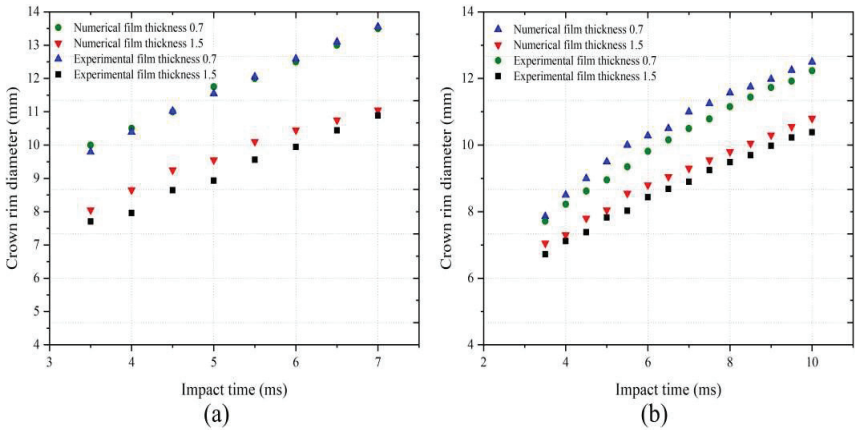

Figure 6 Crown rim diameter development vs. impact time at different experimental and numerical film thicknesses; (a) water and (b) surfactant-water mixture cases; droplet diameter and the Weber number are d = 3.15 mm, and We = 249 (u = 2.4 m/s) for case (a) and d = 2.47 mm and We = 404 (u = 2.4 m/s) for case (b), respectively.

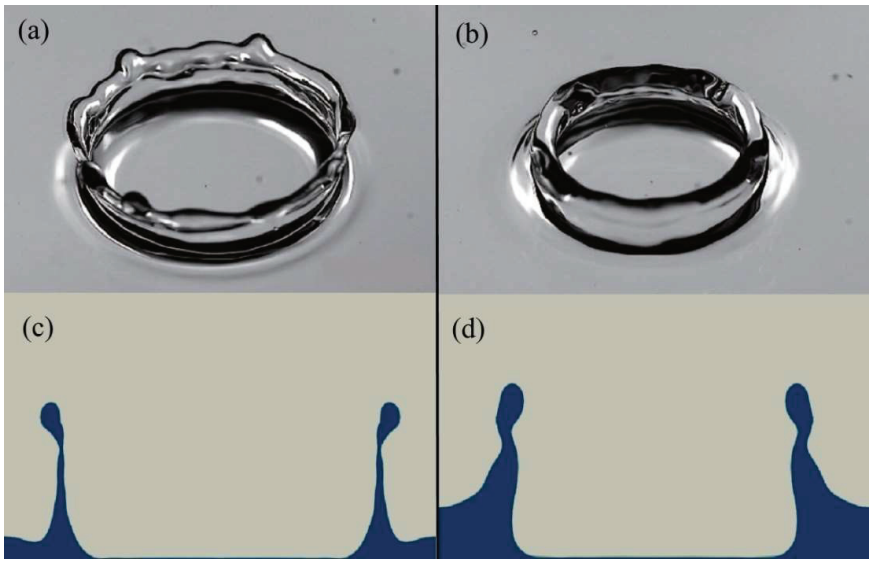

Figure 7 Effect of film thickness on crown formation for water case; a snapshot of crown formation at t = 7 ms after impact; (a) experimental case with the film thickness of h = 0.7 mm (b) experimental case with a film thickness of h = 1.5 mm (c) numerical case with a film thickness of h = 0.7 mm (d) numerical case with the film thickness of h = 1.5 mm; droplet diameter and Weber number are d = 3.15 mm and We = 249 (u = 2.4 m/s), respectively.

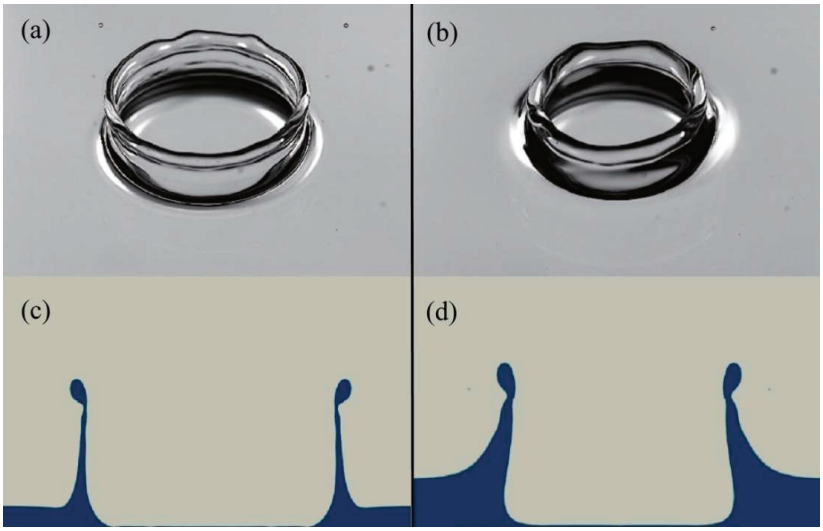

Figure 8 Effect of film thickness on crown formation for surfactant-water mixture case; a snapshot of crown formation at t = 7 ms after impact; (a) experimental case with the film thickness of h = 0.7 mm (b) experimental case with a film thickness of h = 1.5 mm (c) numerical case with a film thickness of h = 0.7 mm (d) numerical case with the film thickness of h = 1.5 mm; droplet diameter and Weber number are d = 2.47 mm and We = 404 (u = 2.4 m/s), respectively.

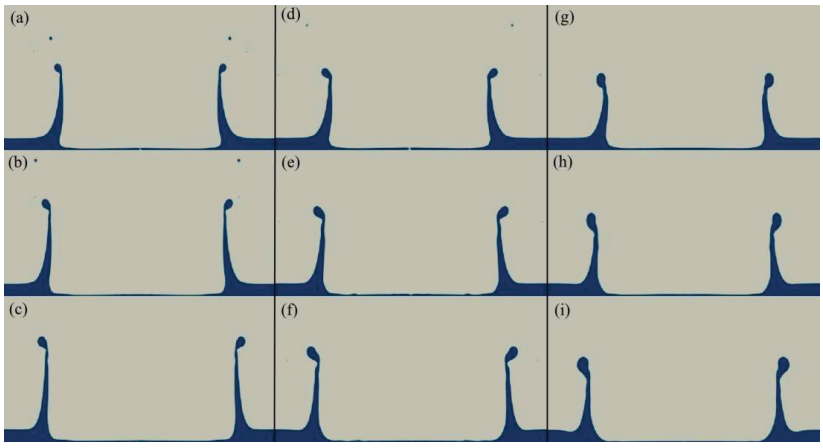

Figure 9 Crown formation snapshot of surfactant-water mixture (a)–(c) surface tension: 0.0344; (d)–(f) surface tension: 0.0520 and (g)–(i) surface tension: 0.0700 at 4, 5, 6 (ms). Droplet diameter and film thickness and impact velocity for the three cases are d = 3.15 (mm), h = 0.7 (mm), u = 2.4 (m/s), respectively.

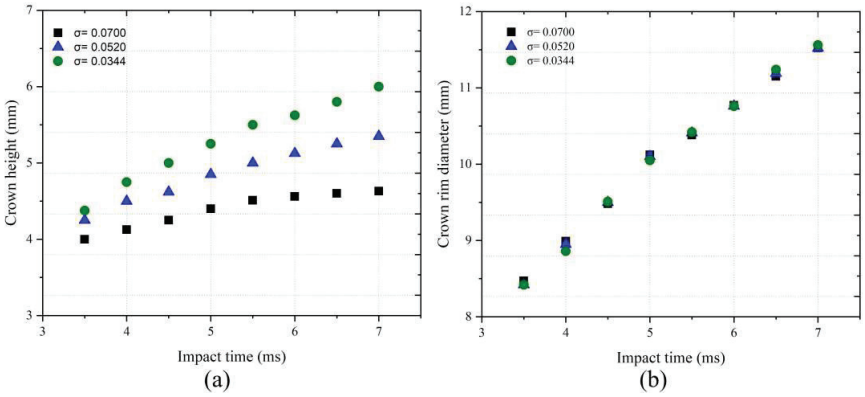

Figure 10 Crown height vs. impact time for three different cases of surface tension coefficients.

crown height against the impact time. The crown height increases as surface tension decreases. It can be seen that the highest Crown is created at the surfactant-water mixture with the lowest surface tension coefficient. Crown height in the third case (g)–(i) is the lowest since it has the largest surface tension coefficient. Figure 10(b) demonstrates the crown rim progress through the impact time. The crown rim diameter evolution does not change with the surface tension, and it is entirely independent of the surface tension [22].

To decipher the underlying process, the energy balance equation is written for droplet and fluid film before and after the impact during the crown formation. Droplet's initial energy is [23]:

$$E_{drop} = KE_i + SE_i = \frac{\rho\pi d^3 u^2}{12} + \sigma\pi d^2 \tag{13}$$

Where KE_i and SE_i are droplet kinetic energy and surface energy, respectively. For drop case with initial parameters of $d = 3.15$ *(mm)*, $u = 2.4$ *(m/s)* and $\sigma = 0.07$ *(n/m)*, these energies can be calculated as:

$$KE_i = 471.08\times10^{-7}(\text{J}), \quad SE_i = 21.80\times10^{-7}\ (\text{J})$$

The surface energy of the droplet is less than %5 of its total energy (E_{drop}). Thus, it is a reasonable assumption to neglect the surface energy in the three droplet case studies:

$$E_{drop} \cong KE_i \tag{14}$$

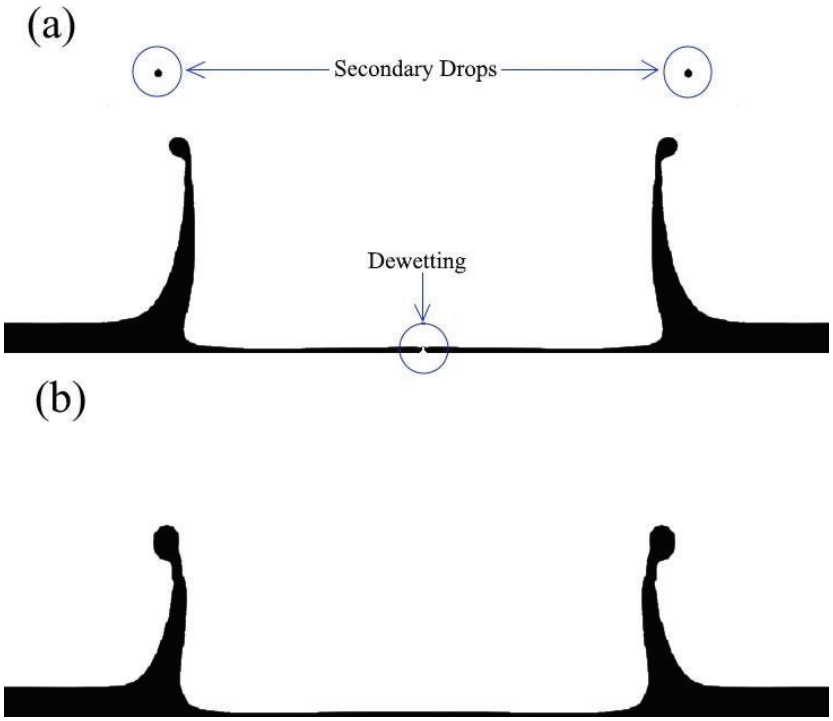

Figure 11 Droplet impact and crown formation for cases with (a) $\sigma = 0.0344$ (b) $\sigma = 0.0700$; at t = 4 (ms) after impact. Secondary droplet and de-wetting region can be seen for the case with low surface tension.

After the impact and during the final stage of crown formation, the droplet's kinetic energy will transform into four different forms of Crown and fluid film's kinetic energy (KE_C), Crown gravitational potential energy (PE_C), Surface energy of Crown and fluid film (SE_C) and Viscous dissipation through the liquid film (DE).

$$E_{final} = KE_C + PE_C + SE_C + DE \tag{15}$$

The Crown's gravitational potential energy has been reported to be less than %3 of the initial total energy and logically negligible [24]. Thus, the final stage of the energy equation can be written as:

$$E_{final} = E_{drop} = KE_i = KE_C + SE_C + DE \tag{16}$$

$$KE_C = KE_i - SE_C - DE \tag{17}$$

Equation (17) describes the relationship between different forms of energy transformation during the crown evolution. Given that KE_i and DE are constant, crown surface energy (SE_C) is controlling the crown kinetic energy. Consequently, in lower surface tension cases, surface energy decreases and Crown's kinetic energy proliferates, and crown height subsequently is elevated.

At low surface tensions, the formation of secondary droplets and surface de-wetting happens at earlier stages because surface tension cannot resist the kinetic energy at the top of crown rims, and secondary droplets are eventually ejected from the crown rim (Figure 11). Hence, in situations where de-wetting and secondary droplets are problematic for a system, surface tension must be high enough in order to omit these unwanted outcomes.

4 Conclusions

A CFD model has been carried out to study the droplet impact and crown formation outcomes. Crown height and rim diameter are explored in different situations. The effect of different Weber numbers and film thicknesses has been discussed. The surface tension effect is also investigated by adding a surfactant to dio-ionized water in order to reduce the surface tension of water while keeping the other properties constant. Weber's number plays a significant role in the crown formation. It is described as the ratio of inertia to surface tension. A higher Weber number (higher velocity) means higher inertia, leading to a larger crown rim and heights. Crown rim diameter increases with the Weber number in both water and surfactant-water cases.

Crown forms faster in thinner liquid films due to the lower resistance of the thinner liquid film. In the thicker film cases, the secondary droplets disappear. This behavior comes from the fact that the thicker liquid films lead to thicker crown rims. Rim diameter escalates as film thickness elevates. Surface energy is noted to be the controlling factor of kinetic energy in crown evolution. Thus, at lower surface tensions, the kinetic energy of the crown rim surges and creates higher crowns.

Nonetheless, crown rim diameter does not changed, suggesting the constant radial inertia for various surface tensions. For low values of surface tensions, secondary drops and de-wetting areas started at an earlier stage of post-impact. Thus, in order to avoid the de-wetting and secondary droplets surface tension must be high enough to resist the crown's kinetic energy. A threshold can also be computed considering the energy balance equation in future research works.

References

[1] X. Tang, A. Saha, C. K. Law, and C. Sun, "Bouncing-to-Merging Transition in Drop Impact on Liquid Film: Role of Liquid Viscosity Bouncing-to-Merging Transition in Drop Impact on Liquid Film: Role of Liquid Viscosity," 2018.

[2] M. Pegg, R. Purvis, and A. Korobkin, "Droplet impact onto an elastic plate: a new mechanism for splashing," pp. 561–593, 2018.

[3] S. L. Manzello and J. C. Yang, "An experimental study of a water droplet impinging on a liquid surface," *Exp. Fluids*, vol. 32, no. 1, pp. 580–589, 2002.

[4] R. Rioboo et al., "Evolution of the ejecta sheet from the impact of a drop with a deep pool," *Phys. Rev. Lett.*, vol. 35, no. January, pp. 580–589, 2013.

[5] L. V Zhang, J. Toole, K. Fezzaa, and R. D. Deegan, "Evolution of the ejecta sheet from the impact of a drop with a deep pool," 2011.

[6] F. Marcotte et al., "Ejecta , Corolla , and Splashes from Drop Impacts on Viscous Fluids To cite this version: HAL Id: hal-02172306," *Phys. Rev. Lett.*, vol. 122, no. 1, p. 14501, 2019.

[7] Z. Che and O. K. Matar, "Impact of droplets on liquid films in the presence of surfactant Impact of droplets on liquid films in the presence of surfactant," *Langmuir*, 2017.

[8] T. Tran, H. De Maleprade, C. Sun, and D. Lohse, "Air entrainment during impact of droplets on liquid surfaces," *J. Fluid Mech.*, vol. 726, pp. 1–11, 2013.

[9] H. Xie, S. Koshizuka, and Y. Oka, "Modelling of a single drop impact onto liquid ÿlm using particle method," vol. 1023, no. June 2003, pp. 1009–1023, 2004.

[10] Y. Guo, Y. Lian, M. Sussman, Y. Guo, Y. Lian, and M. Sussman, "Investigation of drop impact on dry and wet surfaces with consideration of surrounding air Investigation of drop impact on dry and wet surfaces with consideration of surrounding air," vol. 073303, 2016.

[11] G. Agbaglah, M. Thoraval, S. T. Thoroddsen, and L. V Zhang, "Drop impact into a deep pool: vortex shedding and jet formation," no. Worthington 1882, pp. 1–11, 2014.

[12] Y. Guo, L. Wei, G. Liang, and S. Shen, "Simulation of droplet impact on liquid fi lm with CLSVOF ⋆," vol. 53, pp. 26–33, 2014.

[13] D. L. Sun and W. Q. Tao, "International Journal of Heat and Mass Transfer A coupled volume-of-fluid and level set (VOSET) method for

computing incompressible two-phase flows," *Int. J. Heat Mass Transf.*, vol. 53, no. 4, pp. 645–655, 2010.

[14] F. Ommi and G. Heidarinejad, "Numerical analysis of droplet impact onto liquid film," no. January, 2014.

[15] I. Chakraborty, G. Biswas, and P. S. Ghoshdastidar, "International Journal of Heat and Mass Transfer A coupled level-set and volume-of-fluid method for the buoyant rise of gas bubbles in liquids," *HEAT MASS Transf.*, vol. 58, no. 1–2, pp. 240–259, 2013.

[16] S. Asadi and M. Passandideh-fard, "A Computational Study on Droplet," *Arab. J. Sci. Eng.*, vol. 34, no. 2, pp. 505–517, 2009.

[17] T. Xavier et al., "Toward direct numerical simulation of high speed droplet impact To cite this version: HAL Id: hal-02299033 Toward direct numerical simulation of high speed droplet," 2019.

[18] E. Miller and J. Cooper-white, "Journal of Non-Newtonian Fluid Mechanics The effects of chain conformation in the microfluidic entry flow of polymer – surfactant systems," vol. 160, pp. 22–30, 2009.

[19] M. S. Hossain, A. C. Sarker, T. Khandaker, K. Hasan, and N. Khan, "Volumetric and viscometric studies of sodium dodecyl sulphate in aquous and in amino acid solutions at different temperatures," vol. 9, no. 1, pp. 30–41, 2016.

[20] A. B. Aljedaani, C. Wang, and A. Jetly, "Experiments on the breakup of drop-impact crowns by Marangoni holes," *J. Fluid Mech.*, vol. 844, pp. 162–186, 2018.

[21] J. Liu, H. Vu, S. S. Yoon, R. Jepsen, and G. Aguilar, "Splashing Phenomena During Liquid Droplet Impact," *At. Sprays*, vol. 20, no. 4, pp. 297–310, 2010.

[22] C. Peng, X. Xu, and X. Liang, "Numerical investigation on crown behavior and energy evolution of droplet impinging onto thin film," *Int. Commun. Heat Mass Transf.*, vol. 114, no. April, p. 104532, 2020.

[23] A. I. Fedorchenko and A. Wang, "On some common features of drop impact on liquid surfaces," vol. 1349, no. 2004, 2012.

[24] W. C. Macklin, G. J. Metaxas, and W. C. Macklin, "Splashing of drops on liquid layers Splashing of drops on liquid layers," vol. 3963, no. 1976, pp. 1–9, 2014.

Biographies

Mohammad Mehdi Zamani Asl received bachelor's degree in Mechanical Engineering from Shahid Chamran University of Ahvaz in 2017 and currently pursuing his Master's degree in Mechanical Engineering. Since 2016, Mehdi started his research with a specific focus on computational fluid dynamics and multiphase flows and the development of numerical solvers for simulation of flow transport phenomena.

Zahra Dastyar is a PhD candidate in mechanical engineering at Shahid Chamran University of Ahvaz. She received a bachelor's degree as well as master's degree in mechanical engineering at the same university. Her field during master degree was numerical investigation of fluid flows and she is currently working on numerical simulation of multiphase flow. She is interested in different aspects of numerical flow simulation in industrial equipment, separation of multiphase flow and computer-aided design.